AD-A162 791 HIGH REPETITION RATE ELECTRON BEAM RF-ACCELERATION AND SUB-MILLIMETER WAV. (U) CALIFORNIA UNIV LOS ANGELES SCHOOL OF ENGINEERING AND APPLIED. N C LUHMANN ET AL. 1/1

UNCLASSIFIED 14 AUG 85 N00014-84-K-0569 F/G 20/5 NL

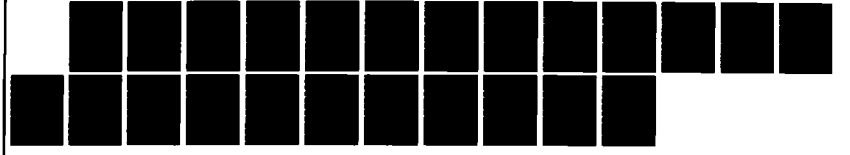

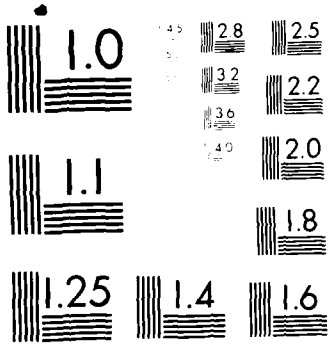

ANNUAL PROGRESS REPORT

1. ONR Proposal Number: P-5610-N-84

2. Period Covered by Report: 15 August, 1984 - 14 August, 1985

3. Title of Proposal: High Repetition Rate Electron Beam RF-Acceleration and Sub-Millimeter Wave Generation via a Free Electron Laser

4. Contract or Grant Number: N00014-84-K-0569

5. Name of Institution: University of California, Los Angeles

SCHOOL OF ENGINEERING AND APPLIED SCIENCE
LOS ANGELES, CALIFORNIA

6. Author(s) of Report: N.C. Luhmann, Jr. and D.B. McDermott

7. List of Manuscripts Submitted or Published under ONR Sponsorship During This Period, Including Journal References:

(a) D.B. McDermott and N.C. Luhmann, Jr., "A High Repetition Rate Compact FEL," Bulletin of the American Physical Society 29, 1180 (1984).

(b) D.B. McDermott, W.J. Nunan and N.C. Luhmann, Jr., "A High Repetition Rate, Compact Free Electron Laser," to be published in Proc. of 1985 IEEE IEDM Meeting.

(c) D.B. McDermott, W.J. Nunan and N.C. Luhmann, Jr., "A High Repetition Rate, Compact Free Electron Laser", to be published in Proc. of Tenth Int. Conf. on IR and mm-Waves.

(d) W.J. Nunan, D.B. McDermott and N.C. Luhmann, Jr., "A High Repetition Rate, Compact Free Electron Laser," submitted to Twenty-Seventh Annual Meeting of the Div. of Plasma Physics.

8. Scientific Personnel Supported by This Project and Degrees Awarded During This Reporting Period: Prof. N.C. Luhmann, Jr.

Dr. D.B. McDermott

W. Nunan (Ph.D. Student)

✓

PER LETTER

A-1

I. THEORY

A. Accelerator

An RF linac has been constructed at UCLA which is specifically designed for FEL applications. The shunt resistance is moderate, thereby allowing the acceleration of relatively high beam currents ($\gtrsim$ 1 A) which will result in moderate FEL gains ($\gtrsim$ 10 dB).

Numerical simulation of the single-cavity TM_{010} linear accelerator has been performed to determine the optimum cavity length. For this value, optimally phased electrons cross the cavity in one half of the rf cycle. This length is dependent on both the input and desired output energies. For the calculations, 10 kV was chosen as the input electron energy and 725 kV as the output energy in order to amplify 94 GHz radiation with a 3.0 cm period wiggler.

The energy of electrons emitted during the RF cycle from a cavity with a length to radius ratio of 0.87 is shown in Fig. 1(a) for an RF power times loaded cavity quality factor of $PQ_L = 3.4 \times 10^9$ W. The dimensionless quantity A is defined by

$$A = (eE/m_o\omega c) \tag{2}$$

where E is the amplitude of the RF electric field and e and m_o refer to the electron's charge and mass, respectively. The corresponding instantaneous current is shown in Fig. 1(b). Injecting a continuous electron beam into the accelerator would result in a time averaged electron beam with a 100% spread in energy. The integrated distribution function of the beam is shown in Fig.

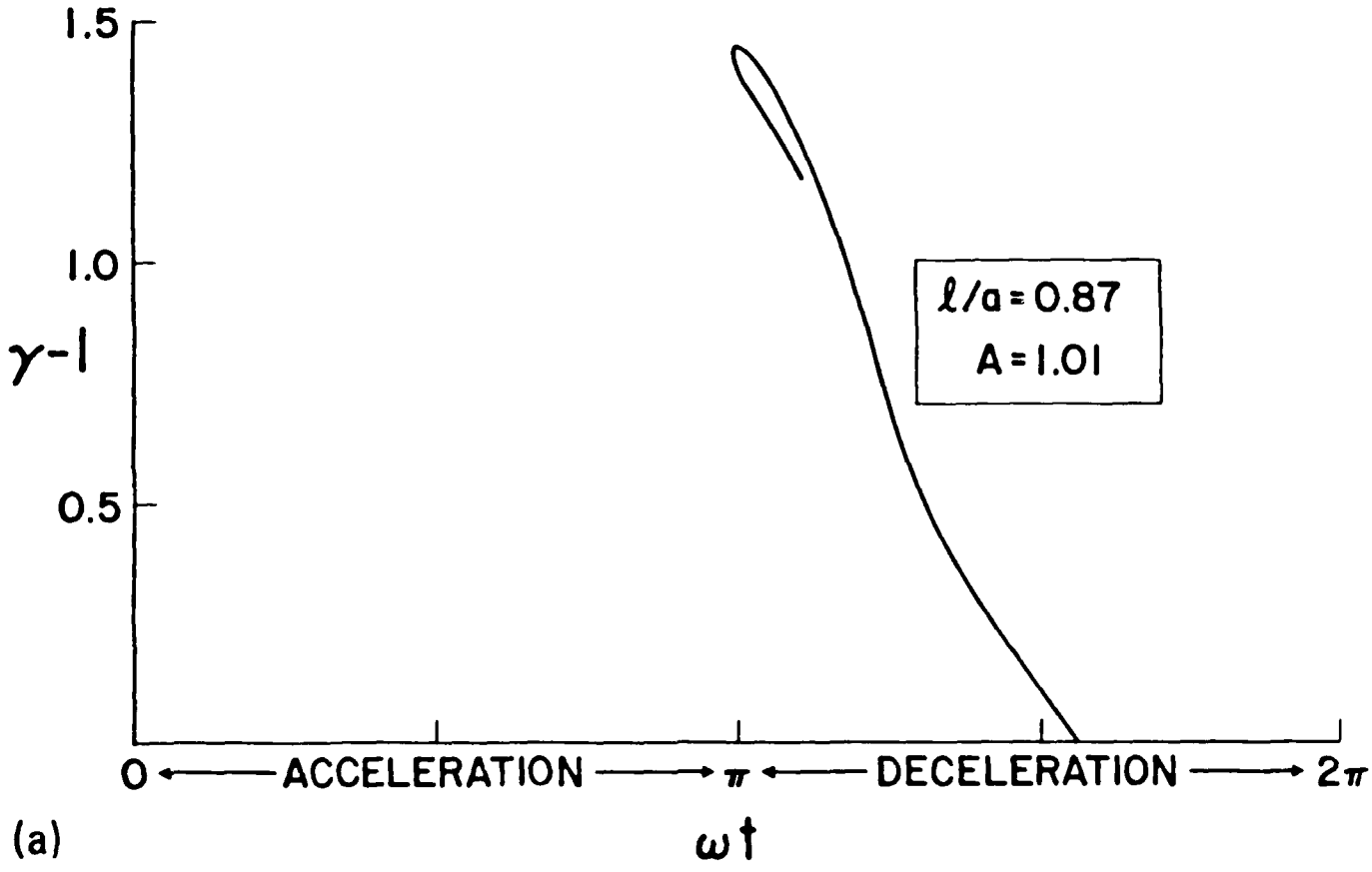

Figure 1 Time history of the a) energy and b) output electron beam current, normalized to the input current, at the accelerator exit.

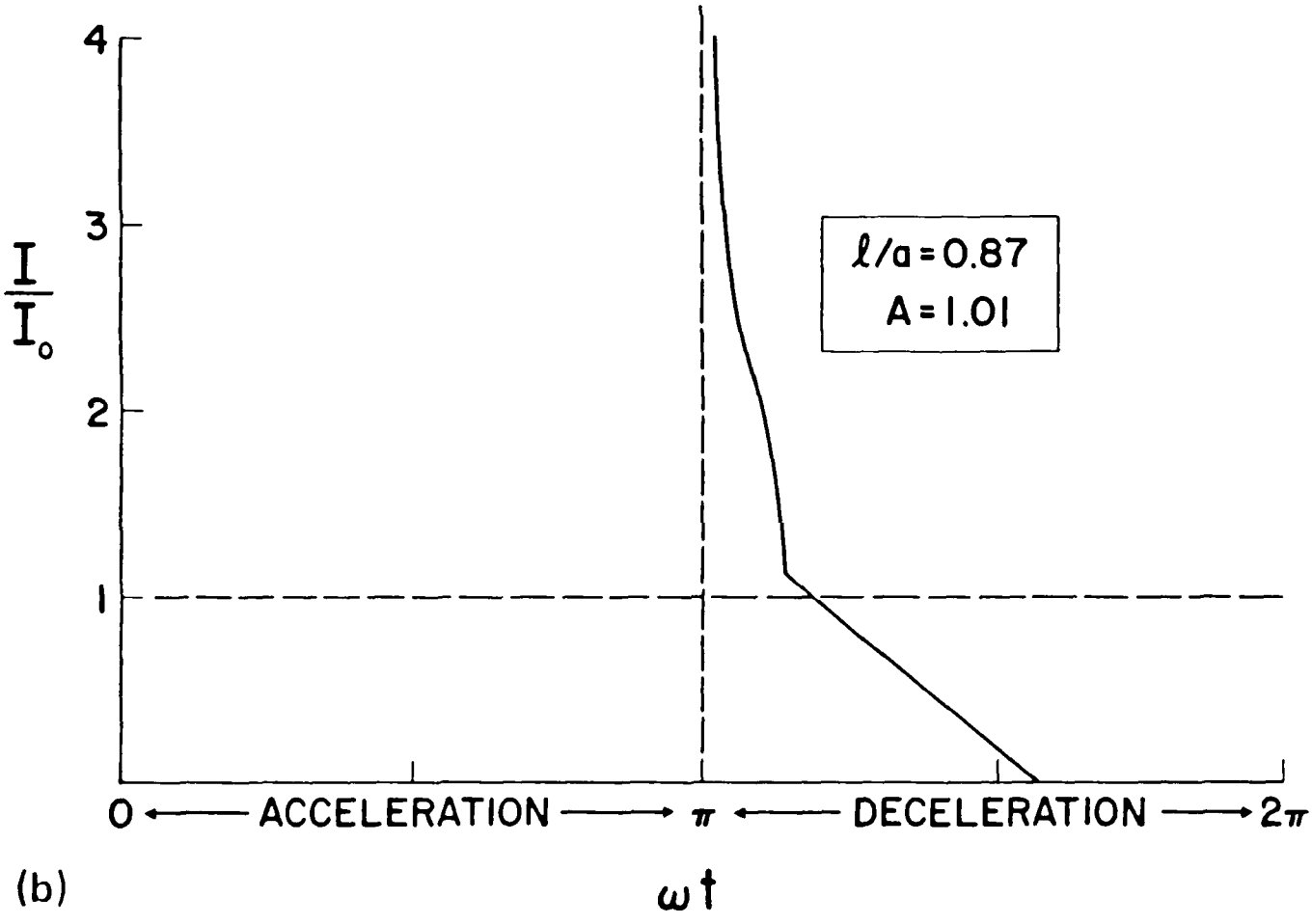

Figure 1 Time history of the a) energy and b) output electron beam current, normalized to the input current, at the accelerator exit.

2(a). Only 6% of the beam is accelerated to within 1% of the peak energy. This situation is inappropriate for FEL applications. By using a buncher cavity similar to a conventional klystron buncher, the electron beam quality can be improved by an order of magnitude.

The integrated distribution function of a tenuous electron beam bunched prior to the accelerator is shown in Fig. 2(b). The quantity ξ, defined by

$$\xi = \omega_q/\omega\alpha \tag{3}$$

is a measure of the beam's repulsive force normalized to the gap's impulsive force, where ω_q is the effective plasma frequency[1], ω is the RF frequency, and α and X are the usual modulation index and bunching parameter, respectively, encountered in klystron theory. Unfortunately, space-charge repulsion during bunch formation will limit the current to several amperes. The integrated distribution function of the more dense, accelerated, bunched beam envisioned for our FEL is shown in Fig. 2(c). In this case 60% of the beam is accelerated to within 1% of the peak energy.

The dependence of the spread in output energy on the thickness of the input pencil beam and magnetic field gradients has also been studied. Basically, as shown in Fig. 3, an off-axis electron will be accelerated as a function of radius as J_o (2.405 r/a), which is also just the dependence of the electric field. An electron beam with a radial spread as large as 1 cm in a 1.3 GHz cavity will emerge with an energy spread of 0.5% due to the radial dependence of the rf electric field and off-axis rf magnetic fields. A gradient in the DC magnetic field is inconsequential.

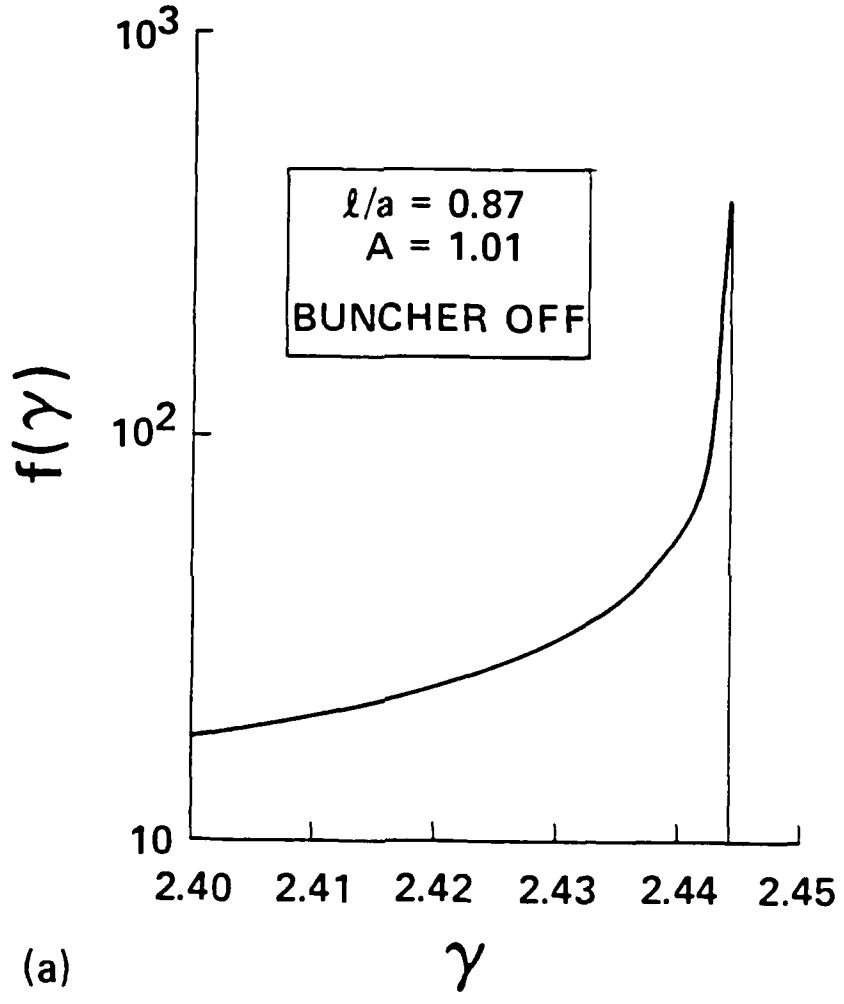

Figure 2 Integrated distribution function a) without buncher, b) with buncher modulating a tenuous beam and c) the more dense beam envisioned for the experiment.

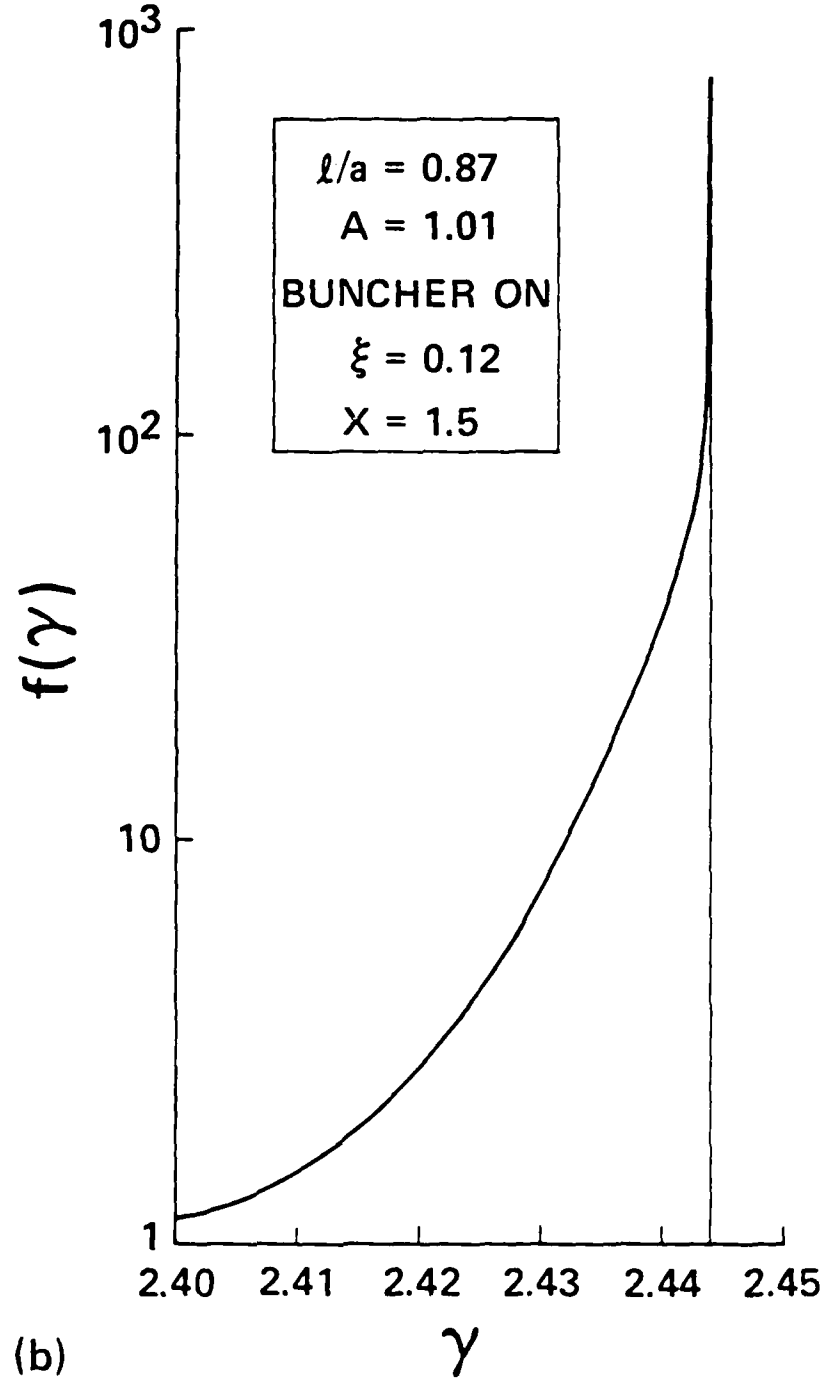

Figure 2. Integrated distribution function a) without buncher, b) with buncher modulating a tenuous beam and c) the more dense beam envisioned for the experiment.

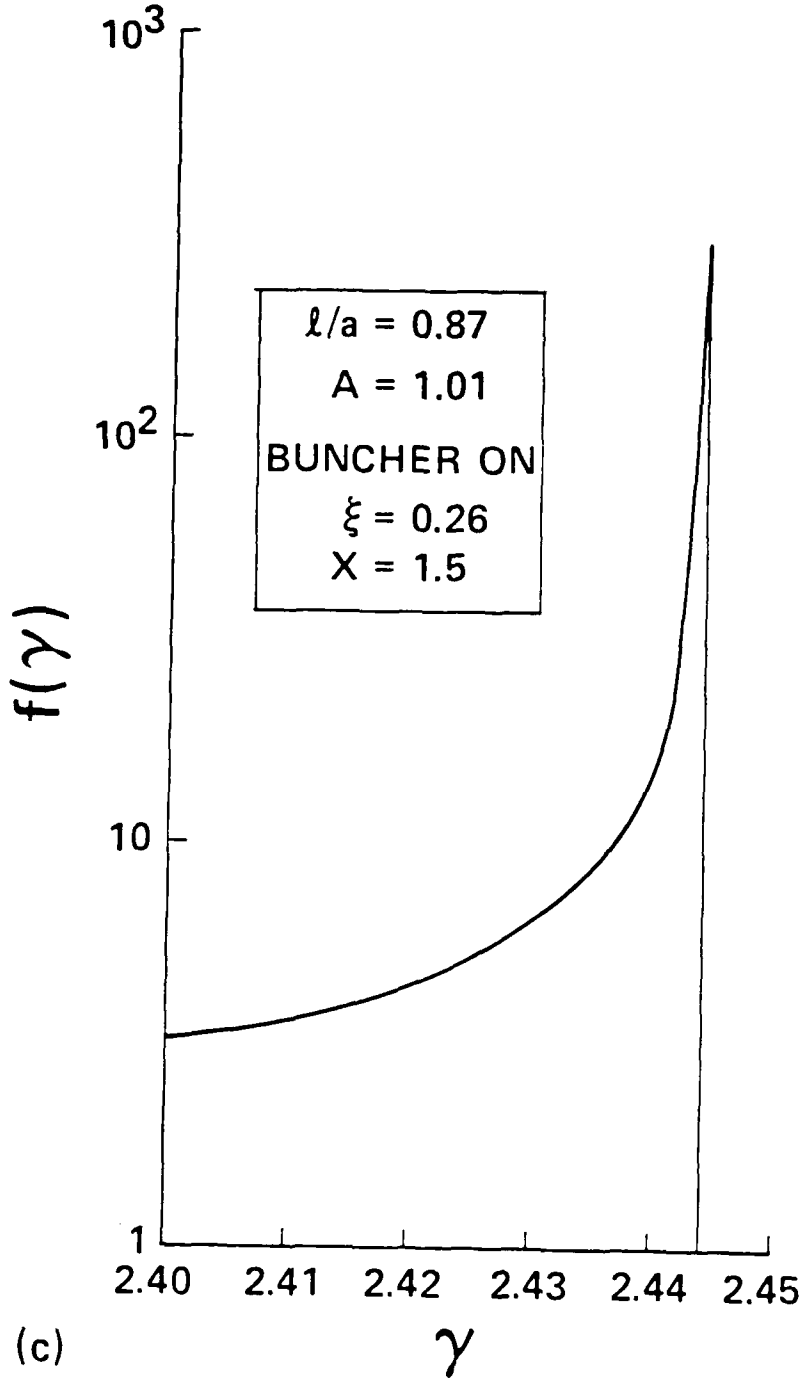

Figure 2. Integrated distribution function a) without buncher, b) with buncher modulating a tenuous beam and c) the more dense beam envisioned for the experiment.

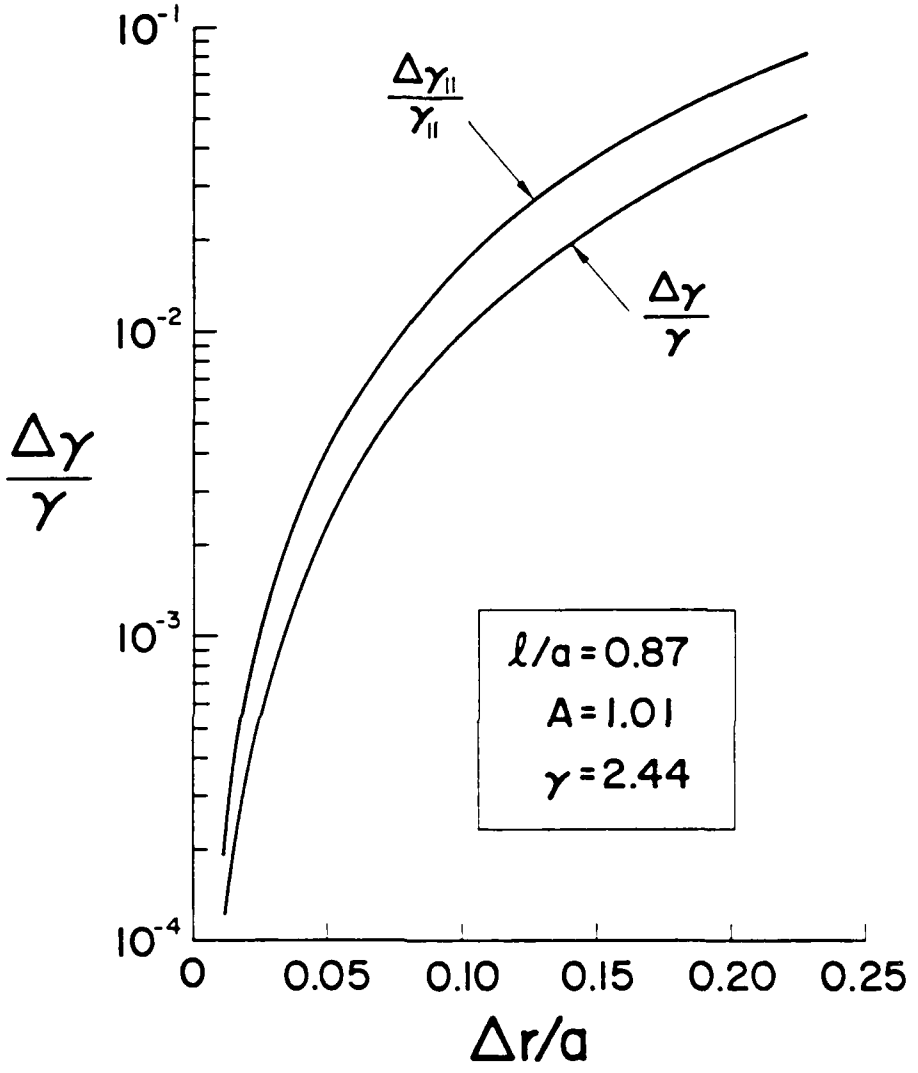

Figure 7. Radial dependence of particle energy.

A gradient in the "pump wave" leads to a gradient in the perpendicular "quiver" velocity and therefore a gradient in the longitudinal velocity, which can lead to competing absorption effects. The periodic transverse magnetic field within a helical wiggler has a radial dependence of $I_o(2\pi r/\ell)$ where is the periodicity. The field will thus vary by 2.5% across a beam with an outer radius of 0.05ℓ. For a monoenergetic beam the spread in longitudinal $\gamma_{\|}$, $\Delta\gamma_{\|}$, can be written in terms of the spread in perpendicular velocity, $\Delta\beta_{\perp}$, as

$$\Delta\gamma_{\|} / \gamma_{\|} = \beta^2 \gamma_{\|}^2 \, (\Delta\beta_{\perp} / \beta_{\perp})$$

A beam with a $\gamma_{\|} = 2.5$ and $\beta_{\perp} = 0.14$ (pump field = 1.5 kG) will have $\Delta\gamma_{\|} / \gamma_{\|}$ equal to an acceptable 0.4% with the previously discussed pump gradient of 2.5%.

The spread in longitudinal velocity of our electron beam, a crucial parameter for any FEL, will be determined by : 1) the gradient in the quiver velocity due to the radial extent of the beam within the inhomogeneous helical magnetic undulator; 2) the energy perturbation induced in the buncher cavity; and 3) the accelerator itself. The energy spread from each of these terms is 0.5%, which results in a total energy spread of 1%.

The beam quality can be improved further by using a multi-cavity linac designed considering the theory of phase stability. The advantage of a standing-wave linac over a travelling-wave linac is that the phase of each cavity can be independently controlled. The beam can thereby be "shaped." The relative phases of the individual cavities should be adjusted so that an electron with the time dependent "synchronous" energy will enter each cavity as the accelerating field is increasing. An electron with energy in excess of

the synchronous value leaving a cavity at the synchronous phase will enter the next cavity earlier than the synchronous phase and therefore will be accelerated less strongly than a synchronous electron. Using the same argument, an electron with less energy than the synchronous value will gain more energy than a synchronous electron. This results in a desirable bunching in momentum space and also in phase space. We have begun to numerically simulate a multicavity linac to determine the minimum number of cavities necessary to achieve a high quality electron beam. A multi-cavity linac can also be used to accelerate particles to much higher energy. Keeping the total RF input power and cavity dimensions constant, the particle energy increases as the square root of the number of cavities.

B. FEL INTERACTION

The initial FEL experiment will be the amplification of 94 GHz output from a 10 W cw (extended interaction oscillator) EIO channeled into the interaction tube through a circulator. The predicted FEL gain for 94 GHz, TE_{11} waves as a function of the beam frame mismatch between the pump and scattered frequencies, ω_i, multiplied by the interaction time, τ, is shown in Fig. 4 using the analytic theory of a finite-length FEL presented in Ref. 2 with γ = 2.5, I = 1 A, B = 1.5 kG, d = 3 cm, wiggler length = 1.5 m, an effective interaction area = 0.35 cm^2 for $\Delta\gamma/\gamma = 0$ ($\theta_t = 0$), $1/2\%$ ($\theta_t = \pi$), and the anticipated 1% ($\theta_t = 2\pi$). θ_p, θ_n and θ_t are defined in Ref. 2. Notice that an energy spread of 1% has reduced the maximum gain by 20 dB from the cold beam case.

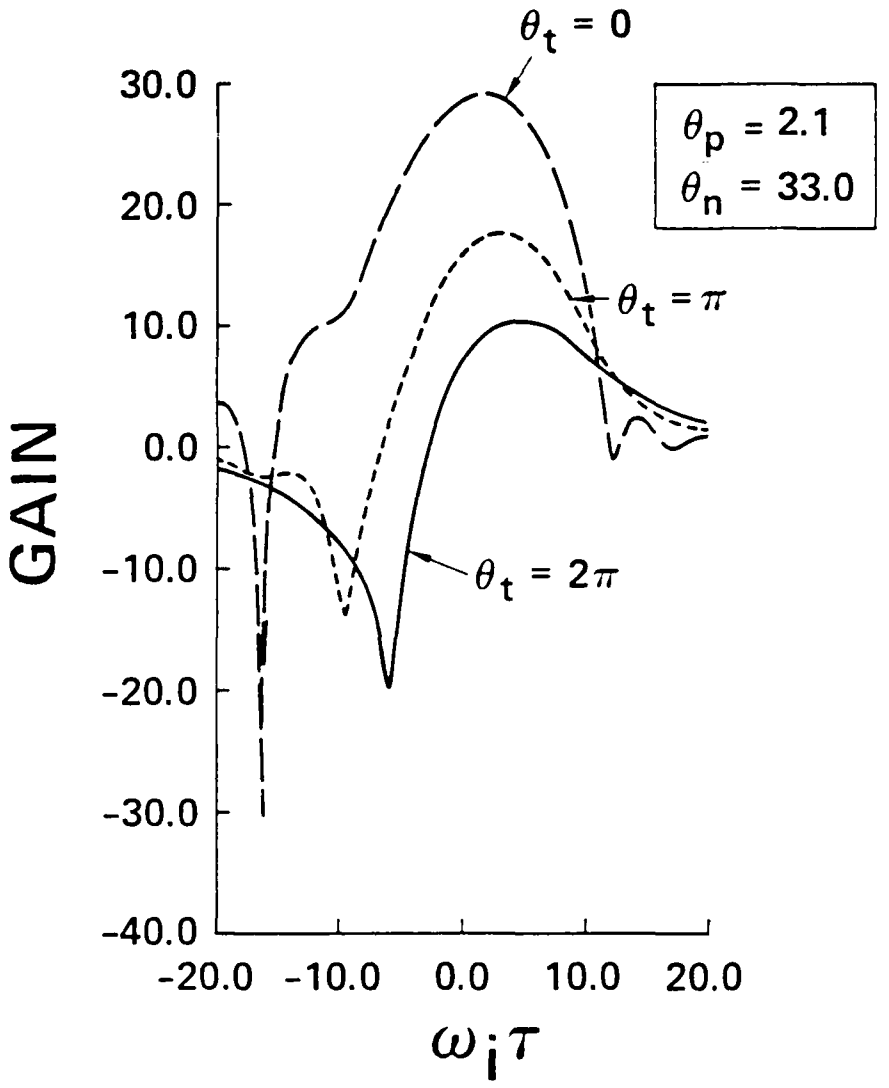

Figure 4 Dependence of gain on the normalized pump-signal mismatch for the anticipated experimental parameters for several values of thermal spread.

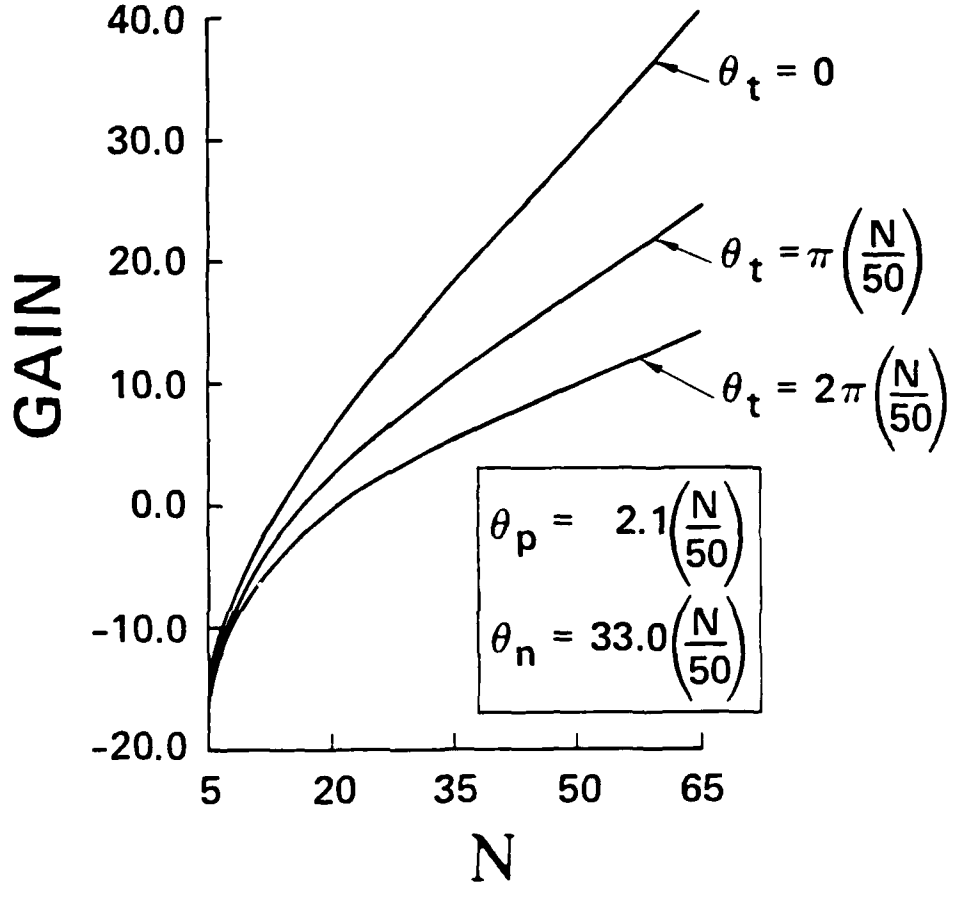

Figure 5. Dependence of gain on the number of unbalanced pairs for the optimized experimental parameters for several values of thermal speed.

The maximum gain as a function of the number of undulation periods is shown in Fig. 5 for our anticipated parameters with three values of thermal spread. For N > 20 the amplitude increases exponentially in space. Both small-signal FEL emission and hot-beam absorption processes are exponential. The net gain is proportional to exp [$(\Gamma_e - \Gamma_a)N$] , where Γ_e and Γ_a are the emission and absorptions constants, respectively. If $\Gamma_e > \Gamma_a$, as for Fig. 5, then gain will increase for a longer undulator. Nevertheless, a gain of 10 dB can still be attained.

During the FEL interaction the electrons with a velocity of approximately 0.9c will quickly slip behind the photons with a group velocity of approximately c. However, this situation is <u>not</u> a problem. Specifically, the monochromatic photons must be treated as waves, not as particles. From another viewpoint, since the frequency linewidth of the FEL gain function, which is less then 1 GHz (< 1% of 94 GHz), is less than the micropulse frequency of 1.3 GHz, RF micropulses can not be emitted, but rather a more nearly continuous macropulse. The production of a very sharp pulse requires a broad Fourier spectrum or a broad gain function. Therefore, the only deleterious effect of our operation with particle/wave slippage is that the gain is determined by the macropulse current and <u>not</u> the peak micropulse current.

Short electron pulses can even enhance FEL gain. First-order effects become dominant as the spatial extent of the electron pulse becomes much shorter than the RF wavelength. Here, all electrons are either accelerated or decelerated in the beat wave of the undulator and RF. This is in contrast to the usual second-order FEL interaction where gain occurs due to a slight dominance of deceleration over acceleration as the energy transfer is integrated

over the initial random particle phase. For this effect to be exploited usefully, the FEL RF driver source must be locked to a harmonic of the accelerator's frequency.

II. EXPERIMENT

Most of the major components for the high repetition-rate, compact rf linac experiment have been assembled and tested. The support table has been constructed. The pressure of the vacuum chamber has been evacuated to below 10^{-8} Torr by a 200 ℓ/s vacion pump aided by a 20 ℓ/s "starter" vacion pump. A filament supply, frequency tuner and coolant system for the high power magnetron (5 MW, QKH 942) have been assembled. The initial 30 kV, 11 MW, 3 μs modulator for the magnetron has been upgraded to 5μs at 40 kV. The voltage ripple is less than 0.5% over 3 μs. The rf system is currently operational and we are "conditioning" the magnetron so that it can operate at its full design value of 5 MW. The magnetron is currently emitting 1 MW.

In order to conveniently test the rf input coupling scheme for the accelerator, a cavity was fabricated which was scaled to S-band (3 GHz). Two coupling geometries were tested. In the first geometry the transverse magnetic field of the waveguide was coupled to the azimuthal magnetic field of the cavity TM_{010} mode by attaching the endwall of the waveguide to the endplate of the cavity with a long narrow slot as the aperture. The measurements of the external quality factor are shown in Fig. 6(a) for the coupling geometry shown in Fig. 6(b). It should be noted that $Q_{ext} = Q_o/\beta_c$, where Q_o is the unloaded quality factor of the cavity and β_c is the coupling coefficient.

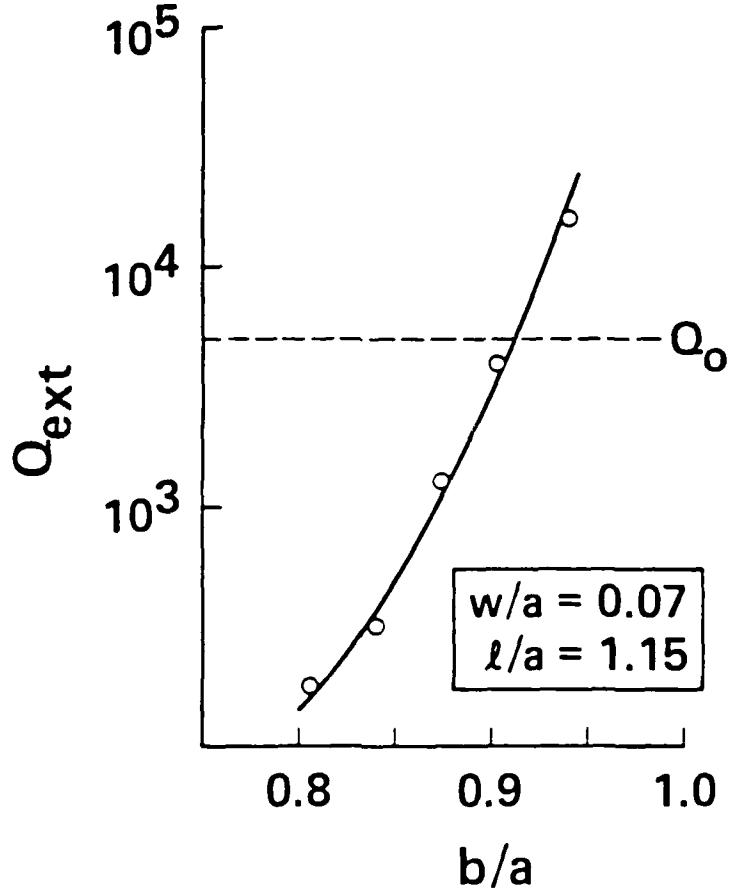

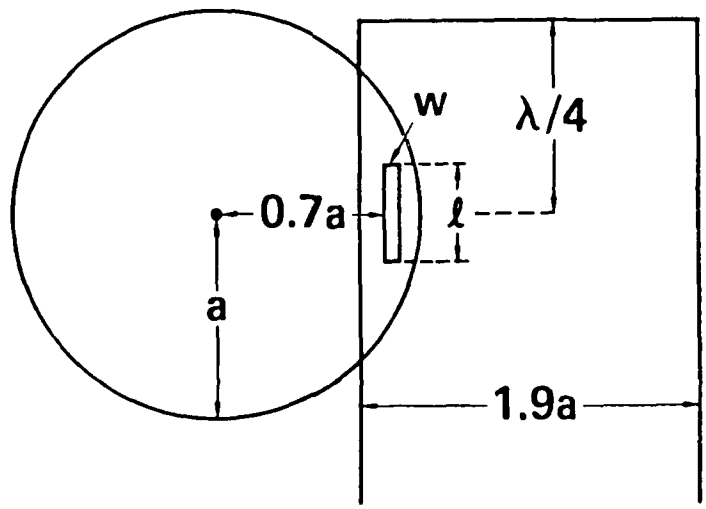

Figure (a) The dependence of the external quality factor on the radial position of the coupling aperture for the waveguide/cavity geometry shown in b). The waveguide terminates on the endplate of the cavity. Q_o is the unloaded quality factor.

It is convenient that overcoupling ($\beta_c > 1$) can be achieved with full-height waveguide. In the second geometry the longitudinal magnetic field of the waveguide was coupled to the azimuthal magnetic field of the waveguide by attaching the broadwall of the waveguide to the endplate of the cavity. The results are shown in Fig. 7(a) for the coupling geometry shown in Fig. 7(b). Again, overcoupling could be easily achieved. However, this last geometry is much more conducive to an expansion in the future of the system into a multi-cavity linac because it requires less space. Therefore, the actual cavity has been constructed with this coupling geometry.

The accelerator and buncher cavities, RF feeds, and drift tubes have been machined. They will soon be brazed and then bolted to the vacuum chamber. For flexibility, the cavities will be sealed by O-rings rather than copper gaskets. The large vacion pump should compensate for the loss of vacuum integrity associated with O-rings.

The electron gun, which was designed to emit up to 5A and withstand 15 kV, hs been constructed. The gun's modulator, power supply, and filament supply have been built and tested. 12 kV, 10μs pulses have been fired into a 500 Ω load, the termination for the delay line. The solenoid has been attached to a large power supply and chilled recirculating water.

The essential diagnostics have been constructed or designed. A Faraday Cup for measurement of beam current, which is mounted on a translatable differentially pumped shaft, has been built. A diagnostic has been designed to measure the degree of bunching of the accelerated beam It will be another TM_{010} cavity with a resonant frequency equal to a high harmonic of the accelerator's frequency. Since a periodic δ- function has infinite Fourier

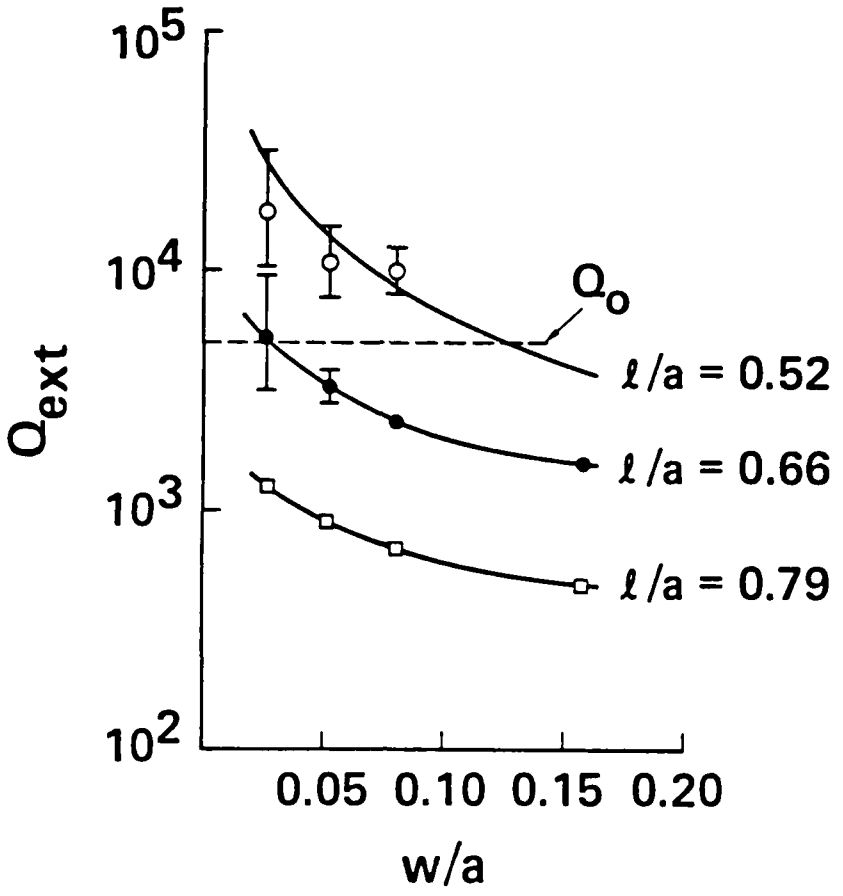

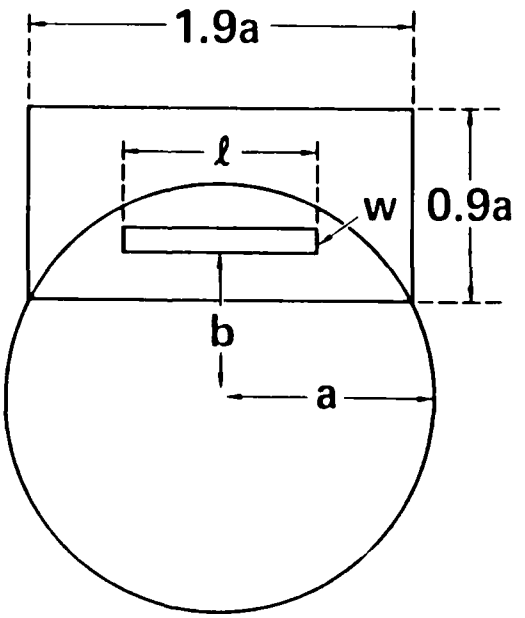

Figure 7 a) The dependence of the external quality factor on the width of the coupling aperture for several values of slot length for the geometry shown in b). The broadwall of the waveguide rests on the end plate of the cavity. Q_o is the unloaded quality factor.

components, the output power from the cavity will yield a measure of the extent of bunching. This cavity is similar to a harmonic klystron catcher cavity. The initial diagnostic to determine the electrons' energy will be a NaI scintillator/photomultiplier. A refrigerated system has been made ready. However, a magnetic spectrometer to measure the Larmor radius will eventually be used. It has yet to be machined. The job is queued into our Engineering Machine Shop.

In summary, the entire system will be ready to accelerate electrons to an energy of up to 2 MeV when the conditioning of the magnetron has been completed. In addition, we have begun to construct the undulator system. The machining of a 3 cm period, electromagnetic wiggler with a 0.5 m amplitude taper region and a total length of 2 m has begun. Components for the capacitor bank have been assembled. The 20 W CW, 94 GHz EIO is scheduled for delivery at the end of October, 1985.

REFERENCES

1. S.E. Webber, Trans. IRE ED -5, 98 (1958).

2. D.B. McDermott, Int. J. IR and mm-Waves 4, 1015 (1983).

FIGURE CAPTIONS

Figure 1 Time history of the a) energy and b) output electron beam current, normalized to the input current, at the accelerator exit.

Figure 2 Integrated distribution function a) without buncher, b) with buncher modulating a tenuous beam and c) the more dense beam envisioned for the experiment.

Figure 3 Radial dependence of particle energy.

Figure 4 Dependence of gain on the normalized pump-signal mismatch for the anticipated experimental parameters for several values of thermal spread.

Figure 5 Dependence of gain on the number of undulation periods for the anticipated experimental parameters for several values of thermal spread.

Figure 6 a) The dependence of the external quality factor on the radial position of the coupling aperture for the waveguide/cavity geometry shown in b). The waveguide terminates on the endplate of the cavity. Q_o is the unloaded quality factor.

Figure 7 a) The dependence of the external quality factor on the width of the couping aperture for several values of slot length for the geometry shown in b). The broadwall of the waveguide rests on the endplate of the cavity. Q_o is the unloaded quality factor.

END

FILMED

7-85

DTIC